Anomalous Metallic State Driven by Magnetic Field at the $LaAlO_3/KTaO_3$ (111) Interface

Zi-Tao Zhang(张子涛), Yu-Jie Qiao(乔宇杰), Ting-Na Shao(邵婷娜), Qiang Zhao(赵强), Xing-Yu Chen(陈星宇), Mei-Hui Chen(陈美慧), Fang-Hui Zhu(朱芳慧), Rui-Fen Dou(窦瑞芬), Hai-Wen Liu(刘海文), Chang-Min Xiong(熊昌民)*, and Jia-Cai Nie(聂家财)*

Department of Physics, Beijing Normal University, Beijing 100875, China

(Received 16 January 2023; accepted manuscript online 17 February 2023)

The origin of the quantum superconductor to metal transition at zero temperature in two-dimensional superconductors is still an open problem, which has caused intensely discussion. Here, we report the observation of a quantum superconductor-to-metal transition in $LaAlO_3/KTaO_3$ (111) interface, driven by magnetic field. When a small magnetic field perpendicular to the film plane is applied, the residual saturated resistance is observed, indicating the emergence of an anomalous metallic state associated with a failed superconductor. The dependence of saturated resistance on magnetic field at low temperature indicates that the observed metal state is a Bose metal state. From our findings, magnetic field regulating $LaAlO_3/KTaO_3$ (111) interface emerges as a platform to scrutinize the details of the anomalous metallic state in a controllable way.

DOI: 10.1088/0256-307X/40/3/037301

When conducting electrons form Cooper pairs in a two-dimensional (2D) disordered system and condense into macroscopic phase coherent quantum states, the global superconductivity will emerge in the sample. According to the conventional theory, when the temperature is close to zero, the superconductor–insulator transition can be observed by applying a magnetic field or disorder.[1–5] The corresponding ground state should be superconducting or insulating state. However, more than 30 years ago, Jaeger *et al.*[2] observed an intermediate metal state which could not be explained by Drude theory when studying ultrathin granular metal films such as Ga, Pb, and In. A hallmark of this intermediate metal state is the existence of saturated residual resistance below the superconducting transition temperature. The relevant superconductor is called "failed superconductor" in the literature.[6] The corresponding ground state is called anomalous metallic state, in which Cooper pairs persist in the metal regime but the phase coherence is lost.

A key signature of the anomalous metallic state is the saturation of resistance with decreasing temperatures, as reported in nanopatterned $YBa_2Cu_3O_{7-x}$ thin films[7] and a 4-monolayer $PdTe_2$ film.[8] The sheet resistance of 4-monolayer $PdTe_2$ film drops and then saturates with decreasing temperatures under a perpendicular magnetic field. Moreover, the use of high-quality filters and linear I–V characteristics demonstrate that the observed anomalous metallic state is intrinsic.[8] Especially, the experimental evidence on bosonic metallic state has been confirmed in nanopatterned $YBa_2Cu_3O_{7-x}$ thin films.[7] In samples with different quantum ground states (superconducting state, anomalous metallic state, and insulating state), the periodic oscillation of resistance with magnetic field is observed, and the period is consistent with one superconducting flux quantum $h/2e$ of Cooper pairs. Besides the $h/2e$ quantum oscillations of Cooper pairs, the zero-Hall coefficient showing particle-hole symmetry also reveals the bosonic nature of anomalous metal state.[7]

In addition to the saturation of resistance at low temperature, the characteristics of anomalous metallic state also include the linear current–voltage (I–V) characteristic in low current range, the giant positive magnetoresistance (MR), and the absence of Hall resistivity. Anomalous metallic state has also been extensively reported in various 2D superconducting systems, such as amorphous films including MoGe films,[9–11] Ta films,[12] TaN_x films,[13] InO_x films,[13] and strongly nonuniform systems like granular films[2,14] and artificially prepared systems like Sn island arrays on graphene[15] and Al square arrays on the InGaAs/InAs heterostructure.[16] It is also observed in mechanical exfoliated crystalline 2D superconductors[17] and the electric-double layer transistors (EDLT).[18,19]

However, studies of the anomalous metallic state at the heterointerfaces between transition metal oxides have been limited in number.[20–23] Recently, 2D superconductivity[23–26] was found in the electronic gas formed at the interface between the (111) oriented $KTaO_3$ (KTO) and the insulating coating of EuO or $LaAlO_3$ (LAO). The superconducting transition temperature of KTO (111) interface system is about one order of magnitude higher than that of $LAO/SrTiO_3$.[27–29] The study of KTO (111)-based interfaces can provide new materials for understanding not only the mechanism of superconductivity but also the origin of the anomalous metallic state in 2D systems. Chen *et al.*[23] reported resistance saturation at the $LaAlO_3/KTaO_3$ (111) interface as the temperature

*Corresponding authors. Email: cmxiong@bnu.edu.cn; jcnie@bnu.edu.cn
© 2023 Chinese Physical Society and IOP Publishing Ltd

decreases, by applying a gate voltage across $KTaO_3$. This suggests the emergence of a quantum metallic state at the $LaAlO_3/KTaO_3$ (111) interface. However, gate voltage always causes irreversible damage to samples. A more reversible and controllable way is needed to tune the system from superconducting into quantum metallic states.

In this work, we observed an anomalous metallic state in LAO/KTO (111) system induced by a magnetic field. A quantum superconductor-to-metal transition (QSMT) was observed by applying a small perpendicular magnetic field. The electrical transport properties were systematically investigated at low temperature and the relationship between the resistance of the anomalous metallic regime and the magnetic field is consistent with the Bose metal model. In addition, the anomalous metallic state emerges in an exceptionally large region of the magnetic field-temperature phase diagram.

The amorphous LAO films were deposited on (111)-oriented KTO substrates by pulsed laser deposition (KrF, $\lambda = 248$ nm) at 760 ℃ in vacuum (7.4×10^{-7} mbar) with a repetition rate of 2 Hz. The fluence of the laser pulses was about 1.5 J/cm^2. After deposition, the samples were cooled *in situ* to room temperature.

The electric contacts were made by ultrasonic wire bonding (Al-wires of 25 μm diameter). The resistance versus temperature and magnetic field was measured in a standard four-probe resistance configuration with a lock-in amplifier (Stanford Research System, SR830) in AC mode in a dilution refrigerator (Triton 400, Oxford Instruments). The frequency of signal was 7.9 Hz. The excitation current was 500 nA for the electrical measurement at temperature from 0.7 K to 2.5 K, and for the ultralow temperature measurement from 750 mK to 40 mK, 100 nA was used. The excitation currents were low enough to avoid Joule heating. For the isomagnetic I–V curves measurement at $T = 100$ mK, current supply and voltage monitoring were controlled by SR830. In our measurements, all applied magnetic fields were perpendicular to the interface. To avoid the influence of high frequency noise in the electrical measurements,[30,31] home-made silver-epoxy filters at ultralow temperature and resistor-capacitor (RC) filters at room temperature were used, which are made similar with those of Wang *et al.*[32] The sample temperature of the dilution refrigerator was calibrated using Co-60 γ-rays in the sub-Kevin region.

The main panel of Fig. 1(a) shows the resistance as a function of temperature for LAO/KTO (111) interface without magnetic field. When the temperature drops below 1.51 K, superconducting transition is observed, with transition temperatures of $T_c^{onset} = 1.51$ K and $T_c^{zero} = 0.72$ K. T_c^{onset} is the temperature where temperatures first deviates from its linear relationship at high temperature, and T_c^{zero} is the temperature at which the resistance drops indistinguishably from the noise floor. We define the resistance at $T = 1.51$ K as the normal resistance R_N. The superconducting transition temperature $T_c = 0.91$ K is defined to be the temperature at which the resistance drops to half of normal resistance value.

Figure 1(b) shows the current–voltage (I–V) characteristics in different magnetic fields at $T = 100$ mK. The appearance of zero resistance state and I–V characteristic provides clear evidence for superconductivity. The inset of Fig. 1(b) shows the I–V characteristics at current below 7 μA. In this region, the linear I–V dependence indicates that the sample has inherent ohmic resistance under the magnetic field greater than 40 mT.

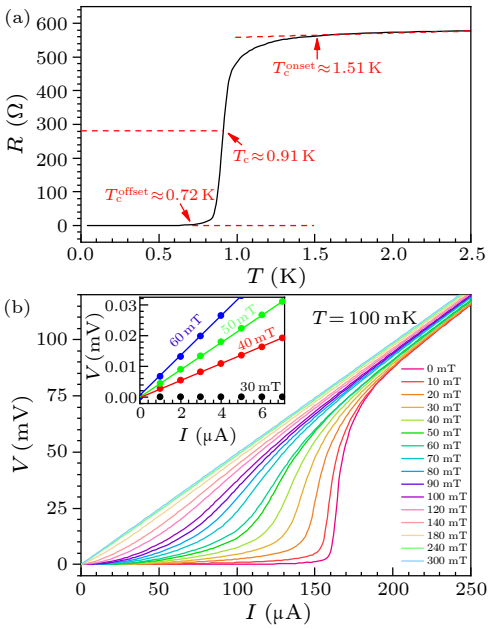

Fig. 1. (a) Resistance with temperature, showing superconducting transition. T_c^{onset}, T_c^{zero}, and T_c marked by red arrows, are 1.51, 0.72, and 0.91 K, respectively. (b) I–V curves at different magnetic field. The inset shows the linear I–V dependences in the low current range. The solid lines are linear fittings.

Figure 2(a) shows the resistance as a function of temperature at magnetic fields applied perpendicular to the film plane, with a QSMT induced by magnetic field. When a small magnetic field is applied, the zero resistance at low temperature disappears, and the residual resistance tends to saturation with the decrease of temperature below the superconducting transition temperature, which is the hallmark of anomalous metallic state. In addition, the saturated residual resistance increases monotonically with the magnetic field. When the magnetic field is greater than 280 mT, the sample is almost in the normal state for all temperatures. The inset in Fig. 2(a) shows a 2D color plot of resistance versus temperature and magnetic field. As mentioned above, we define the temperature-dependent upper critical fields, $H_{c2}^{\perp}$, as the threshold at which the resistance crosses 50% of the normal state value, as shown by black circles in Fig. 2(a).

For clarity, temperature dependence of the resistance with applied magnetic fields ranging from 0 mT to 280 mT is shown in an Arrhenius plot in Fig. 2(b). The resistance saturates to a level, showing the hallmark of the anomalous metallic state when the temperature is approaching to zero (the lowest temperature that can be reached in our experiments is 40 mK. A similar saturation of resistance

for sample 2 was observed in Fig. S3 in the Supplementary Material). The saturation resistance is nearly three orders of magnitude smaller than the value of R_N. The dissipative regime that occurs between the onset of resistance saturation and the normal state shows behavior of thermally assisted flux flow (TAFF):[33]

$$R(T,H) = R_0(H)\exp[-U(H)/k_BT]. \quad (1)$$

Here, $R_0(H)$ is a prefactor, $U(H)$ is the activation energy under field H, and k_B is the Boltzmann constant. The fitting lines are shown in Fig. 2(b) by the black solid lines.

The slopes of the fitting lines in Fig. 2(b) are extracted to obtain the thermal activation energy $U(H)$ and the result is plotted in Fig. 2(c). The dependence of the activation energy on the applied magnetic field is expected as follows:[8,17,33]

$$U(H) = U_0\ln(H_0/H), \quad (2)$$

which is the typical of collective flux creeping. Here, $U_0 = \Phi_0^2 d/(256\pi^3\lambda^2)$ is the vortex-antivortex binding energy, λ is the magnetic penetration depth. The best fitting values of the data are $U_0 = 3.786k_B$ K and $H_0 = 0.113$ T.

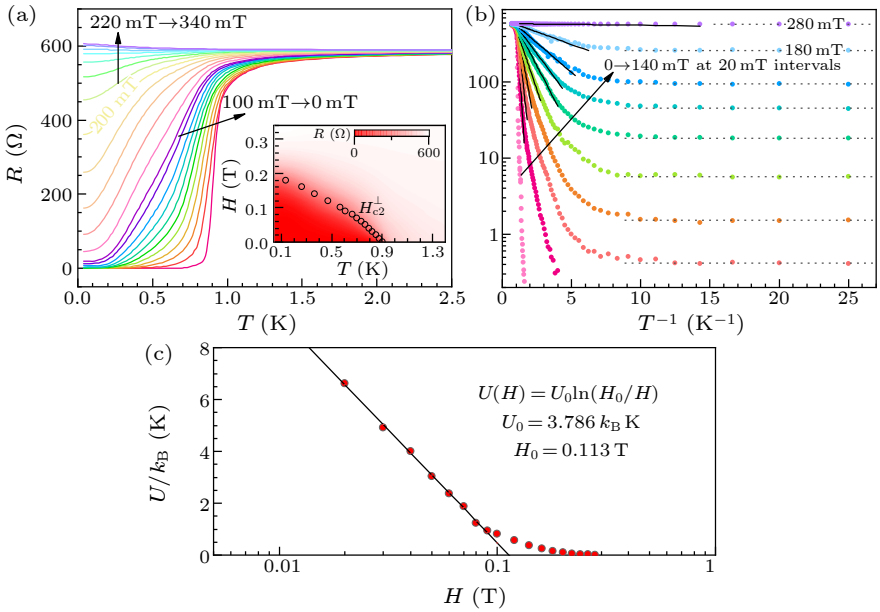

Fig. 2. (a) Resistance versus temperature at different perpendicular magnetic field. The inset shows a 2D color plot of resistance versus temperature and perpendicular magnetic field. The black circles represent the upper critical field $H_{c2}^{\perp}$, defined by $R(H_{c2}^{\perp},T) = 0.5R_N$. (b) Arrhenius plot of resistance for several magnetic fields, showing thermally activated regime (sold lines) and saturation at low temperatures (short dashed lines). (c) Activation energy U/k_B versus magnetic field, extracted from linear fit to activated region. The solid line is empirical fit to formula (2) with $U_0 = 3.786k_B$ K and $H_0 = 0.113$ T.

Figure 3(a) shows the resistance $R(H)$ as a function of magnetic field at different temperatures. As indicated by the black arrow in Fig. 3(a), the isotherm $R(H)$ curves measured at different temperatures cross each other around 0.28 T. The value of this field is comparable with that in Fig. 2(a), which divides the system into normal state and other states. The inset of Fig. 3(a) plots the magnetoresistances MR $= [R(H) - R(H=0)]/R(H=0)$ (where R is the resistance and H is the applied magnetic field) at different temperatures. The giant positive MR in failed superconductor is also one of the characteristics of the anomalous metallic state. We should know that various theories have been proposed before to explain the origin of the dissipation of disordered films in the low temperatures. According to the dependence of saturation resistance on magnetic field at low temperature, different models can be distinguished. The Bose metal model proposed by Das and Doniach[34,35] is a theory widely verified by experiments.[14,17,19] They believe that Cooper pairs exist in both superconducting and anomalous metallic states. When Cooper pairs form a macroscopic phase coherent state, the system behaves as a superconducting state. On the other hand, when the phase coherence of Cooper pairs is lost, the system behaves as an anomalous metallic state.

When a magnetic field is applied, the metal phase is induced by the dynamical gauge field fluctuation caused by the superconducting quantum fluctuation.[35] The uncondensed bosons start to emerge at $H > H_{c0}$, which drives the system into the Bose metal phase, where H_{c0} is the critical field for QSMT. H_{c0} is obtained by the fields where the slope of $R(H)$ curves begins to drop to zero. Figure 3(b) shows a log–log plot of resistance versus $(H - H_{c0})$ at several different temperatures from 0.05 K to 0.5 K. The linear scaling observed here suggests a power-law dependence on field. We have fitted the data to the expression proposed by Das and Doniach:[34,35]

$$R \sim (H - H_{c0})^{2\nu_0}. \quad (3)$$

Near the QSMT and on the metallic side, the resistance scales with $(H - H_{c0})^{2\nu_0}$, where ν_0 is the scaling parameter and it is plotted as a function of temperature in the inset of Fig. 3(b). The fitting results of the formula strongly show that the anomalous metallic state observed in our sample is the Bose metal phase.[14,17,19,34,35]

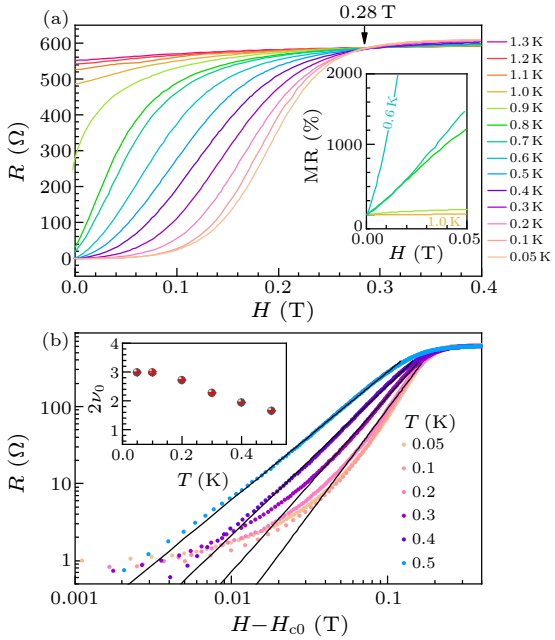

Fig. 3. (a) Resistance versus magnetic field at different temperatures. Inset: MR for LAO/KTO (111). (b) Resistance as a function of $(H - H_{c0})$ in log–log scales at different temperatures. The solid lines are fitting curves, and $2\nu_0$ versus T obtained by fitting is plotted in the inset.

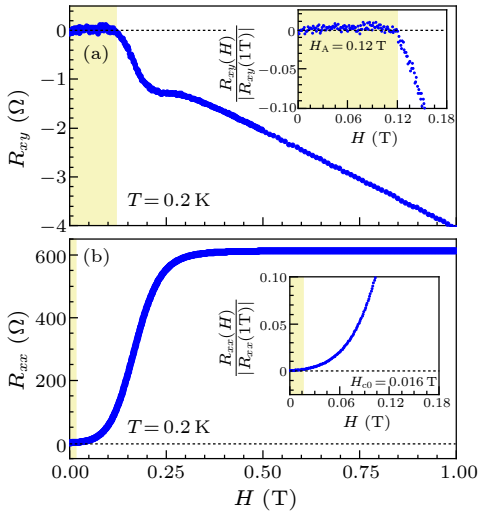

Fig. 4. (a) Transverse resistance as a function of magnetic field at $T = 0.2$ K. Inset: a magnification of the low field data showing normalized transverse resistance. (b) Longitudinal resistance versus magnetic field curves measured at $T = 0.2$ K. Inset: a magnification of the low field data showing normalized longitudinal resistance.

Another hallmark of the anomalous metallic state is abnormal Hall response. Figure 4(a) shows the magnetic field dependence of transverse resistance R_{xy} at $T = 0.2$ K. The slope of $R_{xy}(H)$ curve is largely suppressed and drop to zero below $H_A = 0.12$ T with decreasing magnetic field (Fig. 4(a), inset). Figure 4(b) shows the magnetic field dependence of the longitudinal resistance R_{xx} at $T = 0.2$ K. The inset of Fig. 4(b) shows normalized longitudinal resistance R_{xx}(H)/$|R_{xx}(H = 1\,\text{T})|$, which has a zero-resistance platform approximately below $H_{c0} = 0.016$ T. In brief, at 0.2 K, R_{xy} becomes zero within the measurement resolution at a relatively high magnetic field of ∼0.12 T, whereas R_{xx} is still finite. The absence of Hall resistance at low temperatures reveals the emergence of anomalous metallic state.[7] The observed zero Hall resistance and simultaneously observed giant positive longitudinal MR (Fig. 3(a), inset) further confirmed the existence of the anomalous metallic state.[6]

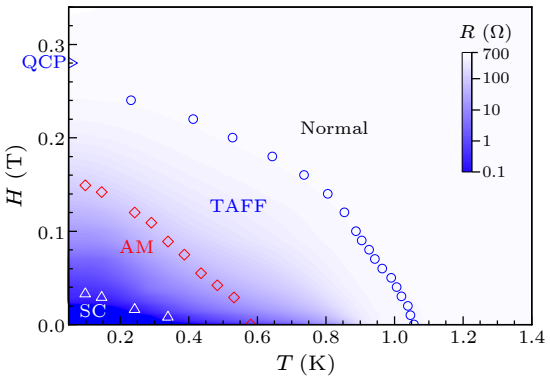

Fig. 5. Full H–T phase diagram of LAO/KTO (111). The background is a 2D color plot of resistance versus temperature and perpendicular magnetic field. The blue triangle around 0.28 T marks the zero-temperature quantum critical point. The blue circles are the locus of points where $R(H, T) = 0.9R_N$ in the isomagnetic curves. The red diamonds, which were obtained from the fields where the slope of $R_{xy}(H)$ curves begin to drop to zero, divide the anomalous metallic state from the TAFF regime. The white triangles are the boundary between superconductor and anomalous metal, obtained from the fields where the slope of $R_{xx}(H)$ curves begin to drop to zero. QCP: quantum critical point. SC: superconductor. AM: anomalous metal.

Figure 5 shows a full H–T phase diagram for LAO/KTO (111). The blue triangle marks the zero-temperature quantum critical point (QCP) obtained by the cross point of isotherm curves in the main panel of Fig. 3(a). The blue circles mark the threshold at which the resistance crosses 90% of the normal state value of isomagnetic $R(T)$ curves in the main panel of Fig. 2(a). They define the boundary between the normal state and other states. The red diamonds between the anomalous metallic state and TAFF mark H_A defined by the fields where the slope of $R_{xy}(H)$ curves [see Fig. S1 in the Supplemental Material)] begin to drop to zero. The white triangles mark H_{c0} defined by the fields where the slope of $R_{xx}(H)$ curves [see Fig. S2 in the Supplemental Material)] begin to drop to zero. In comparison with superconducting state, the anomalous metallic state was observed in a wider range in phase diagram. The results indicate that magnet field

can be used to drive an anomalous metallic state at the $LaAlO_3/KTaO_3$ (111) interface.

In conclusion, we have systematically investigated the low-temperature transport properties of LAO/KTO (111) in perpendicular magnetic field. The R–T curves and I–V characteristics without magnetic field show that the sample is in the superconducting state at low temperature. However, after a small magnetic field is applied, the sample shows the characteristics of resistance saturation at low temperature, linear I–V characteristic, giant positive MR, and abnormal Hall response, indicating the clear characteristics of an anomalous metallic state. The sample undergoes a QSMT at temperature approaching to zero. In short, we have observed the anomalous metallic state in a wide range of magnetic field and our key observations are summarized in the phase diagram. According to the scaling relation for the magnetoresistances at low temperature, we infer that the anomalous metallic state observed in LAO/KTO (111) can be explained by the Bose metal model.

Acknowledgments. This work was supported by the National Natural Science Foundation of China (Grant Nos. 92065110, 11974048, and 12074334), and the National Basic Research Program of China (Grant Nos. 2014CB920903 and 2013CB921701).

References

[1] Goldman A M and Marković N 1998 *Phys. Today* **51** 39
[2] Jaeger H M, Haviland D B, Orr B G, and Goldman A M 1989 *Phys. Rev. B* **40** 182
[3] Fisher M P 1990 *Phys. Rev. Lett.* **65** 923
[4] Hebard A F and Paalanen M A 1990 *Phys. Rev. Lett.* **65** 927
[5] Yazdani A and Kapitulnik A 1995 *Phys. Rev. Lett.* **74** 3037
[6] Kapitulnik A, Kivelson S A, and Spivak B 2019 *Rev. Mod. Phys.* **91** 011002
[7] Yang C, Liu Y, Wang Y *et al.* 2019 *Science* **366** 1505
[8] Liu Y, Xu Y, Sun J *et al.* 2020 *Nano Lett.* **20** 5728
[9] Ephron D, Yazdani A, Kapitulnik A, and Beasley M R 1996 *Phys. Rev. Lett.* **76** 1529
[10] Mason N and Kapitulnik A 1999 *Phys. Rev. Lett.* **82** 5341
[11] Mason N and Kapitulnik A 2002 *Phys. Rev. B* **65** 220505
[12] Qin Y G, Vicente C L, and Yoon J 2006 *Phys. Rev. B* **73** 100505
[13] Breznay N P and Kapitulnik A 2017 *Sci. Adv.* **3** e1700612
[14] He Z H, Tu H Y, Gao K H, Yu G L, and Li Z Q 2020 *Phys. Rev. B* **102** 224502
[15] Han Z, Allain A, Arjmandi-Tash H, Tikhonov K, Feigel'man M, Sacépé B, and Bouchiat V 2014 *Nat. Phys.* **10** 380
[16] Bøttcher C G L, Nichele F, Kjaergaard M, Suominen H J, Shabani J, Palmstrøm C J, and Marcus C M 2018 *Nat. Phys.* **14** 1138
[17] Tsen A W, Hunt B, Kim Y D *et al.* 2016 *Nat. Phys.* **12** 208
[18] Saito Y, Kasahara Y, Ye J, Iwasa Y, and Nojima T 2015 *Science* **350** 409
[19] Li L J, Chen C, Watanabe K, Taniguchi T, Zheng Y, Xu Z, Pereira V M, Loh K P, and Neto A H C 2019 *Nano Lett.* **19** 4126
[20] Chen Z Y, Wang B Y, Swartz A G, Yoon H, Hikita Y, Raghu S, and Hwang H Y 2021 *npj Quantum Mater.* **6** 15
[21] Gupta A, Silotia H, Kumari A, Dumen M, Goyal S, Tomar R, Wadehra N, Ayyub P, and Chakraverty S 2022 *Adv. Mater.* **34** 2106481
[22] Chen Z, Swartz A G, Yoon H *et al.* 2018 *Nat Commun.* **9** 4008
[23] Chen Z, Liu Y, Zhang H *et al.* 2021 *Science* **372** 721
[24] Chen Z, Liu Z, Sun Y *et al.* 2021 *Phys. Rev. Lett.* **126** 026802
[25] Liu C, Yan X, Jin D *et al.* 2021 *Science* **371** 716
[26] Ma Y, Niu J, Xing W *et al.* 2020 *Chin. Phys. Lett.* **37** 117401
[27] Reyren N, Thiel S, Caviglia A D *et al.* 2007 *Science* **317** 1196
[28] Han Y L, Shen S C, You J *et al.* 2014 *Appl. Phys. Lett.* **105** 192603
[29] Monteiro A M R V L, Groenendijk D J, Groen I *et al.* 2017 *Phys. Rev. B* **96** 020504
[30] Tamir I, Benyamini A, Telford E J *et al.* 2019 *Sci. Advances* **5** eaau3826
[31] Xing Y, Yang P, Ge J *et al.* 2021 *Nano Lett.* **21** 7486
[32] Wang P, Huang K, Sun J, Hu J, Fu H, and Lin X 2019 *Rev. Sci. Instrum.* **90** 023905
[33] Feigel'Man M V, Geshkenbein V B, and Larkin A I 1990 *Physica C* **167** 177
[34] Das D and Doniach S 1999 *Phys. Rev. B* **60** 1261
[35] Das D and Doniach S 2001 *Phys. Rev. B* **64** 134511